Int. J. Electrochem. Sci., 13 **(2018)** 12294 – 12310, doi: 10.20964/2018.12.64

International Journal of ELECTROCHEMICAL SCIENCE
www.electrochemsci.org

Monotriazoles Derived from Uracil and Thymine as Corrosion Inhibitor for API 5L X52 Steel in 1 M H_2SO_4

A. Espinoza-Vázquez[1*], *F. J. Rodríguez-Gómez*[1], *Guillermo E. Negrón-Silva*[2], *D. Angeles-Beltrán*[2], *R. González-Olvera*[3].

[1] Facultad de Química, Departamento de Ingeniería Metalúrgica, Universidad Nacional Autónoma de México, C.U., Ciudad de México, C.P. 04510.
[2] Departamento de Ciencias Básicas, Universidad Autónoma Metropolitana-Azcapotzalco Av. San Pablo No. 180 Col. Reynosa-Tamaulipas, México, Ciudad de México., C. P. 02200.
[3]Facultad de Estudios Superiores Zaragoza, Universidad Nacional Autónoma de México, Batalla 5 de Mayo s/n, esquina Fuerte de Loreto, Ciudad de México, C.P. 09230, México.

[*]E-mail: arasv_21@yahoo.com.mx

Received: 28 August 2018 / *Accepted:* 1 October 2018 / *Published:* 5 November 2018

In this study, the corrosion inhibition of monotriazoles derived from uracil and thymine was studied with electrochemical impedance spectroscopy (EIS) on API 5L X52 steel in 1 M H_2SO_4. The addition of compounds diminished the corrosion process of the steel, with MTBU-I and MTBT-Br being the best corrosion inhibition compounds with an η of 91% at 15 ppm. Furthermore, the persistence of the film showed that both compounds are effective up to 48 hours with an η above 90%, and at higher temperatures, the MTBT-Br provides a resistant film over the metallic surface up to 50 °C. Hydrodynamic conditions demonstrated that the MTBT-Br afforded good protection against corrosion up to 100 rpm. According to their Langmuir isotherms, the adsorption process for these molecules is a combination of physisorption and chemisorption. Finally, SEM images show a decrease in the corrosion rate on the metallic surface in the presence of the MTBU-I or MTBT-Br.

Keywords: monotriazoles, API 5L X52, EIS, inhibitor, uracil, thymine

1. INTRODUCTION

Corrosion, in general, is the slow and progressive destruction of a metal by the action of an external agent. One of the factors that limit the life of the in-service metallic pieces is the chemical or physicochemical attack that they suffer by the surrounding environment [1-3].

Sulfuric acid has important applications in oil refining, the production of pigments, the treatment of steel, the extraction of non-ferrous metals and the manufacture of explosives, detergents, plastics and fibers, as well as in the elimination of oxides present on metallic surfaces. However, metals tend to decay during oxide elimination [4-6].

To prevent or decrease the corrosion rate, an organic inhibitor is generally added in very small proportions relative to the corrosive medium. This substance forms a protective, insoluble compound over the metal surface [7-10]. On the other hand, some organic compounds such as pyrazine derivatives [11-12], ionic liquids [13], thiazolo-pyrimidine derivatives [14], nitrile derivatives [15], azole derivatives [16], benzoxazines[17], aminophosphonic derivatives [18], isatin derivatives [19], Schiff bases [20], quinoxaline [21], thiophene derivatives [22], *N*-aminorhodanine [23], diamine derivatives [24], and [*N*-substituted]*p*-aminoazobenzene derivatives [25,26] are reported as corrosion inhibitors for steel in acidic media. However, they require high concentrations (>50 ppm) to achieve inhibition efficiencies (η) as high as 80% under static conditions.

Nevertheless, the 1,2,3-triazoles are members of the azole family and have been broadly used as heterocyclic inhibitors of steel corrosion caused by acid. These compounds display pharmaceutical activities that are less harmful to the environment, such as di-alkyl and di-1,2,3-triazole derivatives of uracil and thymine [27], connected benzyl glycoside-serine/threonine conjugates [28], triazolyl bis-amino acid derivatives [29], triazolyl glycolipid derivatives [30], maleic acid [31], alkyl triazol derivatives [32] and chalcones [33].

Recently, studies on corrosion inhibition using monotriazoles derived from thymine and uracil (Fig. 1) evaluated in 1 M HCl revealed that the compounds exhibited a corrosion inhibition efficiency of ~96% at a 25 ppm concentration [34].

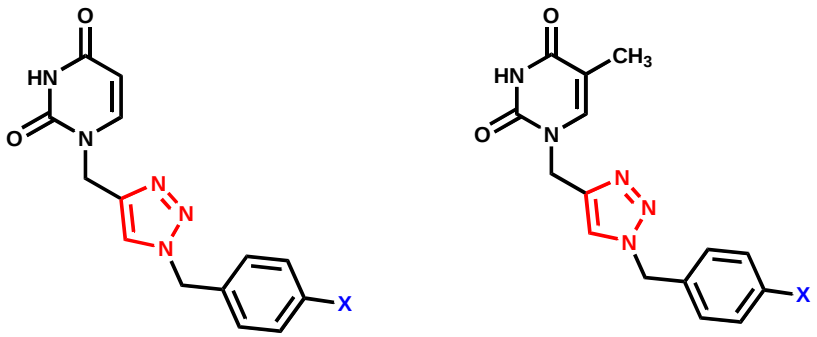

Figure 1. Chemical structures of the compounds evaluated as corrosion inhibitors: a) MTBU and b) MTBT derivatives

Considering the demonstrated effectiveness of these compounds, the objective of this paper is to evaluate the corrosion inhibition properties of monotriazoles derived from uracil and thymine in a sulfuric acid medium, under conditions of laminar flow and different immersion times using electrochemical impedance spectroscopy and scanning electron microscopy (SEM).

2. EXPERIMENTAL

2.1 General synthesis of monotriazoles derived from uracil and thymine

The monotriazoles derived from uracil and thymine are 1-((1-benzyl-1*H*-1,2,3-triazol-4-yl)methyl)pyrimidine-2,4-(1H,3H)-dione (MTBU), 1-((1-(4-fluorobenzyl)-1*H*-1,2,3-triazol-4-yl)methyl)pyrimidine-2,4(1H,3H)-dione(MTBU-F), 1-((1-(4-chlorobenzyl)-1*H*-1,2,3-triazol-4-yl)methyl)pyrimidine-2,4(1H,3H)-dione (MTBU-Cl), 1-((1-4-bromobenzyl-1*H*-1,2,3-triazol-4-yl)methyl)pyrimidine-2,4(1H,3H)-dione (MTBU-Br), 1-((1-(4-iodobenzyl)-1*H*-1,2,3-triazol-4-yl)methyl)pyrimidine-2,4-(1H,3H)-dione (MTBU-I), 1-((1-benzyl-1*H*-1,2,3-triazol-4-yl)methyl)-5-methylpyrimidine-2,4-(1H,3H)-dione (MTBT), 1-((1-(4-fluorobenzyl)-1*H*-1,2,3-triazol-4-yl)methyl)-5-methylpyrimidine-2,4-(1H,3H)-dione (MTBT-F), 1-((1-(4-chlorobenzyl)-1H-1,2,3-triazol-4-yl)methyl)-5-methylpyrimidine-2,4-(1H,3H)-dione (MTBT-Cl), 1-((1-(4-bromobenzyl)-1*H*-1,2,3-triazol-4-yl)methyl)-5-methylpyrimidine-2,4-(1H,3H)-dione (MTBT-Br), 1-((1-(4-iodobenzyl)-1*H*-1,2,3-triazol-4-yl)methyl)-5-methylpyrimidine-2,4-(1H,3H)-dione (MTBT-I). The monotriazoles were prepared via a reaction among the nucleobase of monopropargyl, sodium azide, and several benzyl halides in the presence of a catalytic amount of Cu $(OAc)_2 \cdot H_2O$ in EtOH-H_2O (2:1 v/v) at room temperature for 24 h to provide the desired products with good performance [34].

2.2 Solution preparation

A 0.01 M dissolution of the monotriazoles shown in Fig. 1, which was synthesized and characterized, was prepared and dissolved in dimethylformamide (DMF).

2.3 Steel preparation

API 5L X52 type steel was used with a metallographic preparation of the following composition (wt. %): C, 0.080; Mn, 1.06; Si, 0.26; Ti, 0.003; V, 0.054; Nb, 0.041; P, 0.019; S, 0.003; Al, 0.039; Ni, 0.019; Ceq, 0.274; and Fe, balance [35]. The steel samples employed for the tests using electrochemical impedance spectroscopy had an exposed area of 0.196 cm^2 for the rotating disk.

Specimen preparation included being smoothed down using sandpaper of different grains, up to 1200, polished with Al_2O_3 (1-mm particles), washed with tap water followed by distilled water, degreased with acetone, dried and stored in a desiccator.

2.4 EIS measurements

Gill-Ac equipment was used for the EIS measurements by applying a sinusoidal potential of ±10 mV in with frequency interval from 10^4 to 10^{-2} Hz in a three-electrode electrochemical cell. The working electrode was API 5L X52 steel with an exposed area of 0.196 $cm^{2.}$ The counter electrode was a graphite bar, and the reference electrode was Ag/AgCl saturated with KCl.

A concentration scan was performed by varying the amount of inhibitor from 10 to 200 ppm relative to the corrosive 1 M H_2SO_4 solution.

2.5 Evaluation of the hydrodynamic conditions and immersion time

The best inhibitors of both families derived from thymine and uracil, namely, MTBU-I and MTBT-Br, were evaluated using a rotating disk electrode at 40 and 100 rpm using a Pine Research Instrumentation MSRX module instrument with an exposed area of 0.196 cm^2. The effect of the immersion time was tested by taking measurements from 0.5 hours to 240 hours at 50 ppm.

3. RESULTS AND DISCUSSION

3.1 Effect of concentration

The Nyquist impedance diagram (Z_{re} vs Z_{Im}) in the absence of the inhibitor (Fig. 2) presents only one time constant and is observed to corresponding to the Bode plot related to a charge transfer resistance of ~25 Ω cm^2.

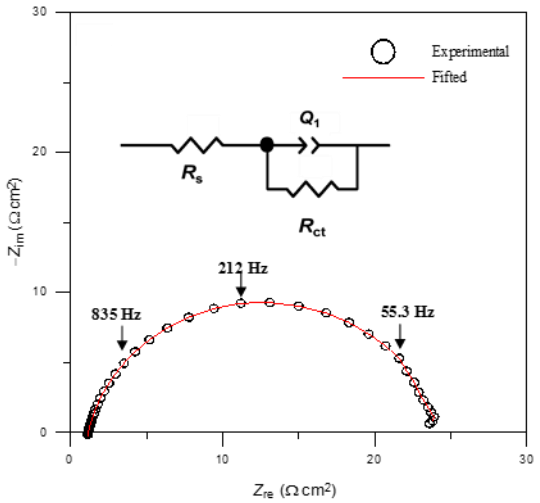

Figure 2. Nyquist diagram of the API 5L X52 steel immersed in 1 M H_2SO_4 at static conditions

The impedance diagrams of the MTBU (Fig. 3a), MTBU-F (Fig. 3b), MTBU-Cl (Fig. 3c) and MTBU-I (Fig. 3e) present two time constants: one related to high frequencies with the charge transfer resistance and the second related to low frequencies with the organic molecule resistance.

However, for the MTBU-Br (Fig. 3d), the system is controlled by the charge transfer resistance since this inhibitor shows a depressed semicircular shape with only one time constant.

The semicircle that has its center under the x axis is characteristic of solid electrodes. The resulting frequency dispersion has been attributed to the roughness and other inhomogeneities of the metallic surface [36-38]. Additionally, the presence of accumulated molecules or corrosion products results in a depression of the semicircles.

In general, it can be observed the diameter of the Nyquist diagrams increases after the addition of the monotriazoles uracil derivatives to the 1 M H_2SO_4. This enhancement is observed when the added structure element is electronegative.

These observations indicate that the adsorption of the monotriazole molecules on the mild steel surface forms a protective film. This film reduces the active sites of the steel and enhances its corrosion resistance [39].

The presence of a halogen element is important to inhibit the corrosion since the heteroatoms with free lone pair electrons promote chemical adsorption. It can be observed at 50 ppm in Fig. 3(a) that the value of Z_{re} is ~218 Ω cm^2. In Fig. 3b, Z_{re} reaches a value of 76 Ω cm^2, which is slightly larger than the semicircle diameter compared with when the molecule lacks the halogen element.

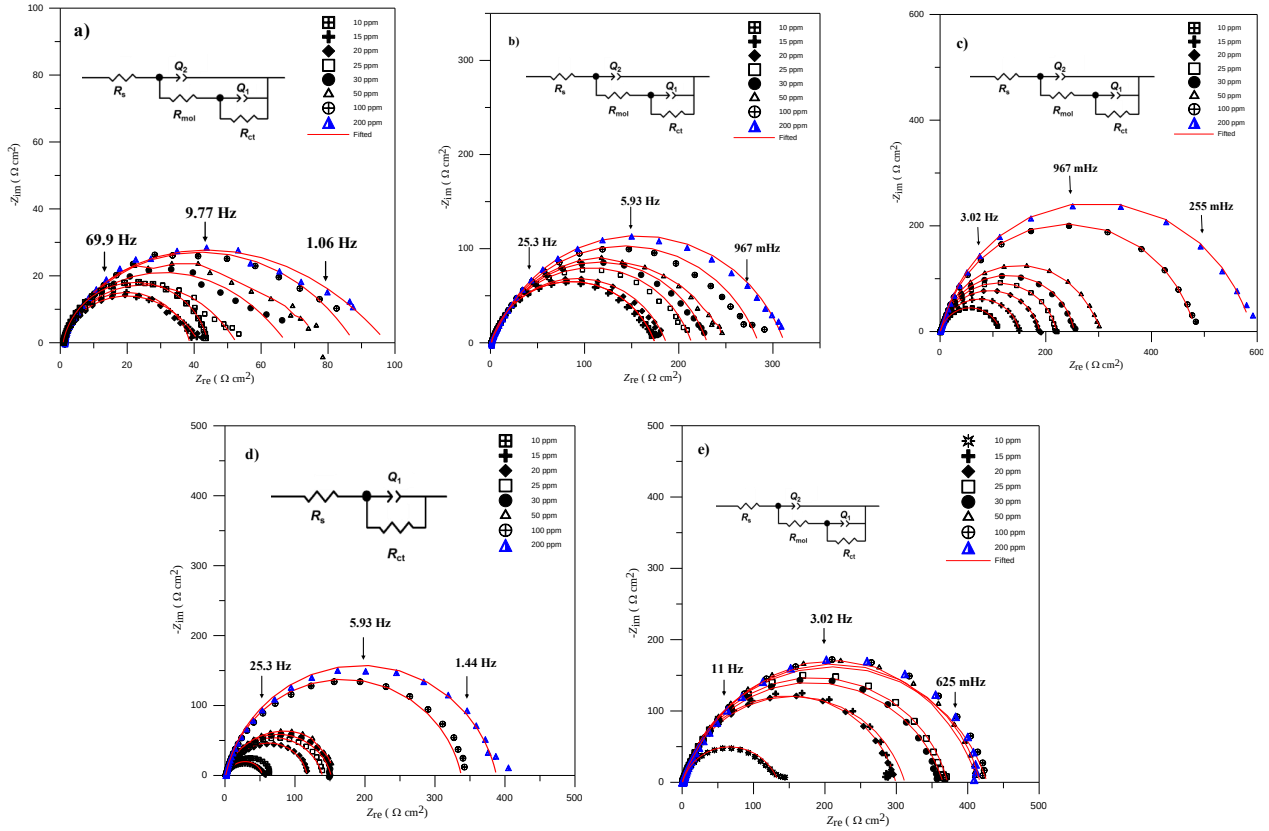

Figure 3. Nyquist diagrams measured as a function of the concentration of a) MTBU, b) MTBU-F, c) MTBU-Cl, d) MTBU-Br, and e) MTBU-I on API 5L X52 steel immerse in 1 M H_2SO_4 at static conditions

The electrochemical parameters of the organic compounds summarized in Fig. 1 were determined using electrochemical impedance spectroscopy and analyzed with the electric circuits shown in the Nyquist plots adjusted with the program Zsim.

To describe the independent phase of the frequency, an applied AC potential is changed, and the response of the current for a constant phase element (CPE) is used to define the impedance representation as:

$$Z_{CPE} = Q^{-1}(j\omega)^{-\alpha} \quad (1)$$

where Q is the pseudo capacitance, ω is the angular frequency in rad s^{-1}, j = -1 is the current density, and α is the CPE exponent. Depending on n, the CPE may represent the resistance (Z (CPE) = r, α = 0), capacitance (Z (CPE) = C, α = 1), the inductance (Z (CPE) = L, α = -1) or the Warburg impedance for (α = 0.5). The CPE parameter Q cannot represent the capacitance when α < 1. In this case, the capacitance is:

$$C_{\mathrm{dl}} = Q^{1/\alpha}(R_{\mathrm{s}})^{1-\alpha/\alpha} \quad (2)$$

where C_{dl} is the double layer capacity and Rs is the solution resistance, which is equivalent to the equation reported by Brug for an ideally polarized electrode [40].

The value of the polarization resistance (R_{p}) can be obtained from the diameter of the semicircle, which contains the charge transfer resistance (R_{ct}) and the organic molecule resistance (R_{mol}).

The inhibition efficiency (η) was calculated using the sum of resistances (Rp) by [41]:

$$\eta\ (\%) = \frac{\left(\frac{1}{Rp}\right)_{\mathbf{Blank}} - \left(\frac{1}{Rp}\right)_{\mathbf{inhibitor}}}{\left(\frac{1}{Rp}\right)_{\mathbf{Blank}}} \text{ x } 100 \quad (3)$$

where $R_{\mathrm{p\ blank}}$ is the polarization resistance in the absence of an inhibitor and $R_{\mathrm{p\ inhibitor}}$ is for when an inhibitor is present

The parameters obtained for each of the different evaluated MTBU derivative inhibitors are shown in Table 1. In each case, the value of the charge transfer resistance increases as the inhibitor concentration increases, and the impedance of the CPE was used to replace the double layer capacitance (C_{dl}) with a more accurate fit, as described below.

The decrease in Q is likely due to a decrease in the local dielectric constant and/or an increase in the thickness of the protective layer at the electrode surface [42]. This would therefore enhance the corrosion resistance of the studied API 5L X52 steel in the 1 M H_2SO_4.

Table 1. Electrochemical parameters of the MTBU derivatives as corrosion inhibitors in API 5L X52 steel immersed in 1 M H_2SO_4 at static conditions

COM-POUND	C (ppm)	R_s (Ω cm^2)	α	Q (S sec^α)	C_{dl} (μFcm^{-2})	R_{ct} (Ω cm^2)	Q (S sec^α)	R_{mol} (Ω cm^2)	η (%)	X^2
Blank	0	1.1	0.8	9.16x10^{-4}	163.2	25	-	-	-	0.0006
MTBU	10	1.3	0.9	3.16x10^{-4}	88.5	37.3	-	-	33.0	0.0077
	15	1.3	0.8	7.77x10^{-4}	209.5	38.3	7.96x10^{-5}	1.9	34.7	0.0067
	20	1.3	1.0	8.90x10^{-4}	890.1	46.4	7.56x10^{-5}	5.5	46.1	0.0066
	25	1.3	1.0	9.53x10^{-4}	952.5	63.5	7.82x10^{-5}	3.0	60.6	0.0074
	30	1.3	1.0	9.80x10^{-4}	979.7	74.9	7.23x10^{-5}	1.9	66.6	0.0068
	50	1.4	1.0	6.81x10^{-4}	634.9	78.4	6.81x10^{-5}	6.5	68.1	0.0059
	100	1.4	1.0	9.24x10^{-4}	806.4	77.0	8.48x10^{-5}	9.7	67.5	0.0059
	200	1.4	1.0	1.03x10^{-4}	964.2	94.8	6.38x10^{-5}	1.5	73.6	0.0065
	10	1.9	1.0	1.94x10^{-4}	37.4	168.3	3.22x10^{-5}	5.179	84.1	0.0011

MTBU-F	15	1.9	0.7	$1.73x10^{-4}$	27.8	167.9	$3.25x10^{-5}$	5.0	83.4	0.0013
	20	1.9	0.7	$1.74x10^{-4}$	28.0	178.7	$3.02x10^{-5}$	7.1	84.8	0.0010
	25	2.0	0.7	$1.80x10^{-4}$	29.6	205.8	$3.10x10^{-5}$	9.3	87.0	0.0009
	30	2.0	0.8	$1.80x10^{-4}$	33.9	218.7	$3.07x10^{-5}$	12.3	88.1	0.0013
	50	2.0	0.7	$1.94x10^{-4}$	33.4	234.0	$3.05x10^{-5}$	14.5	89.0	0.0009
	100	1.9	0.7	$2.02x10^{-4}$	30.3	273.4	$2.99x10^{-5}$	12.8	90.5	0.0016
	200	2.0	0.7	$1.93x10^{-4}$	32.6	292.0	$2.91x10^{-5}$	18.8	91.4	0.0008
MTBU-Cl	10	0.9	0.9	$4.88x10^{-4}$	169.0	114.0	$1.33x10^{-4}$	0.5	78.1	0.0011
	15	1.0	0.8	$4.93x10^{-4}$	88.6	149.0	$4.31x10^{-4}$	91.0	83.2	0.0014
	20	0.9	0.9	$4.82x10^{-4}$	169.4	189.9	$3.35x10^{-3}$	1.0	86.8	0.0021
	25	0.9	0.9	$4.55x10^{-4}$	155.9	218.1	$4.74x10^{-3}$	1.5	88.5	0.0020
	30	0.9	0.9	$4.49x10^{-4}$	148.8	251.3	$8.83x10^{-3}$	2.3	90.1	0.0008
	50	0.9	0.9	$4.39x10^{-4}$	141.2	248.5	$7.13x10^{-3}$	65.8	89.9	0.0008
	100	1.0	0.9	$4.45x10^{-4}$	132.1	419.6	$5.85x10^{-3}$	65.7	94.0	0.0012
	200	1.0	0.9	$4.39x10^{-4}$	128.8	535.4	$9.55x10^{-3}$	58.0	95.3	0.0011
MTBU-Br	10	1.1	0.8	$2.34x10^{-4}$	45.4	65.0	-	-	61.5	0.0016
	15	1.4	1.0	$2.08x10^{-5}$	20.8	57.2	-	-	56.3	0.0058
	20	1.4	0.9	$1.16x10^{-4}$	35.8	104.2	-	-	76.0	0.0013
	25	1.5	0.8	$9.90x10^{-5}$	11.0	138.1	-	-	81.9	0.0043
	30	1.6	0.9	$1.14x10^{-4}$	28.4	149.1	-	-	83.2	0.0012
	50	1.6	0.9	$1.25x10^{-4}$	30.3	157.6	-	-	84.1	0.0021
	100	1.7	0.9	$9.54x10^{-5}$	29.0	288.9	-	-	91.3	0.0103
	200	1.8	0.9	$9.82x10^{-5}$	28.8	348.5	-	-	92.8	0.0019
MTBU-I	10	0.7	1.0	$3.73x10^{-5}$	37.3	130.4	$2.43x10^{-4}$	4.2	80.8	0.0026
	15	0.7	1.0	$6.01x10^{-5}$	36.8	285.0	$1.23x10^{-4}$	13.3	91.2	0.0019
	20	0.7	0.9	$6.93x10^{-5}$	35.6	302.1	$1.40x10^{-4}$	9.5	91.7	0.0018
	25	0.8	0.9	$7.64x10^{-5}$	34.9	354.6	$1.23x10^{-4}$	16.9	92.9	0.0011
	30	0.7	1.0	$5.80x10^{-5}$	34.3	354.1	$1.62x10^{-4}$	11.0	92.9	0.0014
	50	0.8	0.9	$9.31x10^{-5}$	33.7	393.1	$1.02x10^{-4}$	22.2	93.6	0.0013
	100	0.6	0.8	$1.00x10^{-5}$	8.97	404.5	$1.26x10^{-4}$	27.2	93.8	0.0029
	200	1.0	0.8	$1.75x10^{-5}$	2.33	395.9	$6.24x10^{-5}$	29.2	93.7	0.0014

Structurally, the non-halogenated monotriazole derived from the uracil provided a low inhibition to corrosion. Thus, at concentrations up to 50 ppm and higher, the presence of the electronegative halogen atom is an important element to incorporate into the corrosion inhibitors, as shown by the inhibition efficiencies above 90% exhibited by the halogenated monotriazoles.

It has been demonstrated that halide ions inhibit the corrosion of some metals in strong acids and that this effect depends on the size and the ionic charge, as well as on the electrostatic field created by the negative charge of the anion in the adsorption site. This can be attributed to the fact that the radius and the electronegativity of the ions have an influence on the corrosion inhibition [43].

In the case of the monotriazoles derived from thymine (Fig. 4), MTBT-F (Fig. 4b)exhibited a noticeable increase in Z_{re} from 50 Ωcm^2 at 10 ppm up to 200 Ωcm^2 at 15 ppm. However, above this concentration, the Z_{re} gradually increased up to 250 Ωcm^2. In this case, the MTBT (Fig. 4a),

fluorinated (MTBT-F) and iodized (MTBT-I) compounds are controlled by the charge transfer resistance.

The MTBT-Cl (Fig. 4c) showed similar behavior but with a Z_{re} of ~190 Ωcm^2 and the MTBT-Br (Fig. 4d) showed a depressed semicircle attributed to the presence of two time constants, reaching a Z_{re} value of ~600 Ωcm^2. In Fig. 4e, corresponding to MTBT-I, a Z_{re} value of ~300 Ωcm^2 was observed.

Nevertheless, when the compound does not contain any halogen (Fig. 4e), the value of Z_{re} is lower than when halogen is present. The presence of halogens in the chemical structure of the compound is thought to produce a higher availability of electrons. These electrons are able to adhere more easily to the metallic surface since they coordinate with the steel-free electrons from the vacant orbitals [44].

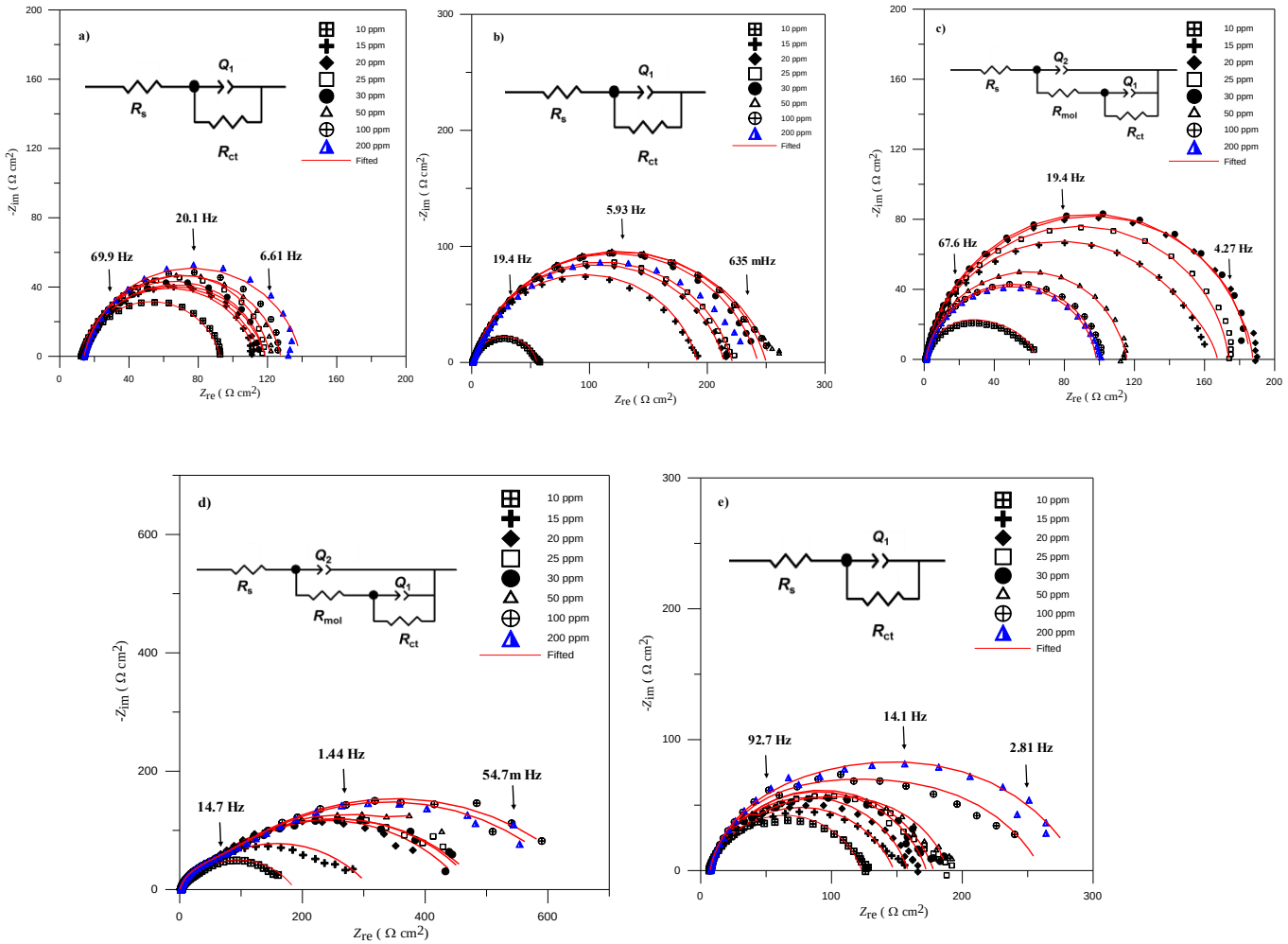

Figure 4. Nyquist diagrams measured as a function of the concentration of a) MTBT, b) MTBT-F, c) MTBT-Cl, d) MTBT-Br, and e) MTBT-I on API 5L X52 immersed in 1 M H_2SO_4 at static conditions

The Bode plots shown in Fig. 5 indicate that the increase in the absolute impedance (log |Z|) at low frequencies confirms the corrosion protection with presence of the inhibitors (Fig. 5a and 5c), which is related to the adsorption of monotriazoles on the surface of API 5L X52 steel. In Fig. 5b, it is noted that there are two coupled time constants, as also noted from the Nyquist plots.

The single peak obtained in Bode plots, see Figs. 5b and 5d, with non-inhibitor (blank) and the presence of MTBU-Br, MTBT, MTBT-F and MTBT-I indicates that the electrochemical impedance measurements were well fit in the one-time constant equivalent model with a constant phase element (*Q*).

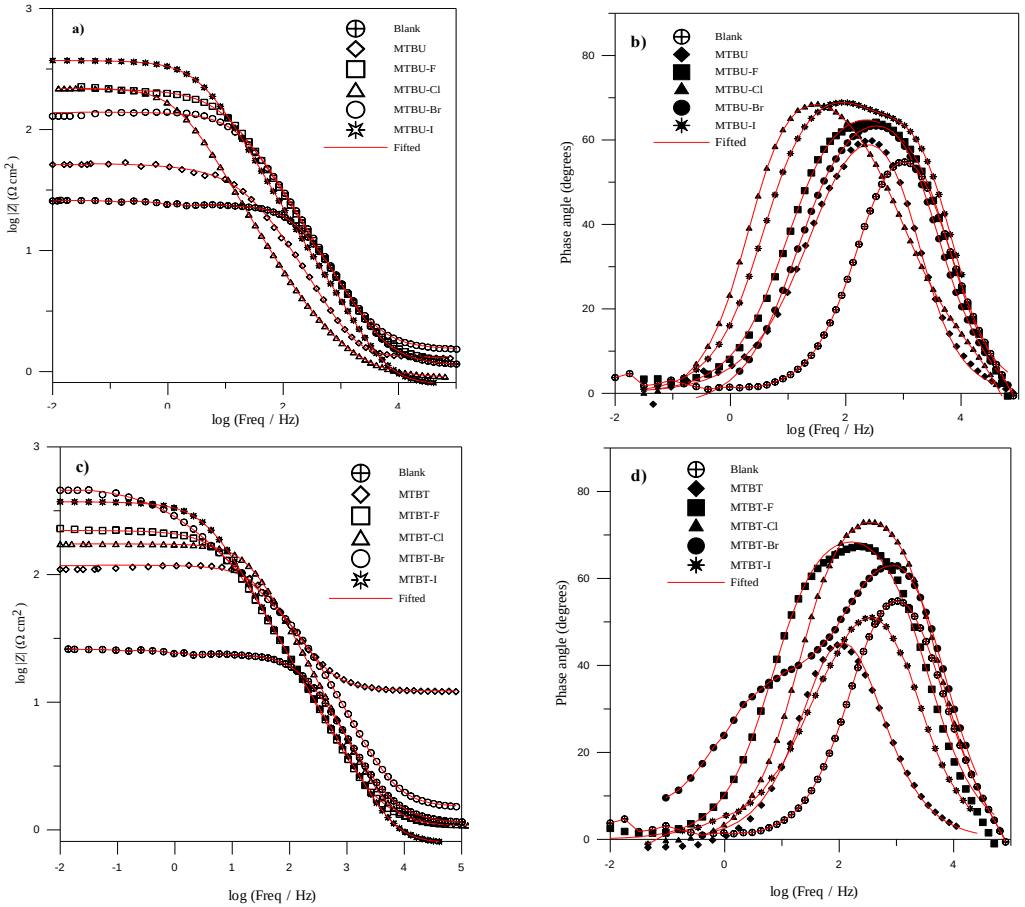

Figure 5. Bode diagrams of a) MTBU and b) MTBT derivatives at 25 ppm on API 5L X52 steel immerse in a H_2SO_4 solution at static conditions

In Table 2, the data obtained from the electrochemical measurements at different inhibitor concentrations are shown. From the MTBT derivatives, it was observed that, similar to the MTBU derivatives, the higher the concentration is, the higher is the inhibition efficiency and the lower is the capacitance of the double layer. This is due to the gradual replacement of water molecules and other ions originally adsorbed on the surface by the adsorption of the inhibitor molecules on the metal surface [45].

The low chi-squared values (X^2) obtained for all the fitting results indicate that the experimental data were effectively fit using the proposed equivalent circuits in Figs. 3 and 4.

On the other hand, it is possible to observe that the best inhibitor compounds at low concentrations (15 ppm) is MTBU-I (η > 91%) and MTBT-Br (η > 92%), while the least efficient compound is the MTBU. Accordingly, these inhibitors are fit to protect the PEMEX ducts.

Table 2. Electrochemical parameters of the MTBT derivatives as corrosion inhibitors in API 5L X52 steel immersed in 1 M H_2SO_4 at static conditions

Compound	*C* (ppm)	R_s (Ω cm^2)	α	*Q* (S sec^α)	C_{dl} (μFcm^{-2})	R_{ct} (Ω cm^2)	*Q* (S sec^α)	R_{mol} (Ω cm^2)	η (%)	X^2
MTBT	10	13.4	0.8	6.42 x10^{-5}	10.9	79.3	-	-	68.5	0.00060
	15	14.0	0.8	8.43 x10^{-5}	15.6	96.2	-	-	74.0	0.00032
	20	14.5	0.9	8.53 x10^{-5}	31.3	101.4	-	-	75.3	0.00035
	25	12.5	0.9	9.24 x10^{-5}	33.6	105.8	-	-	76.4	0.00093
	30	14.7	0.9	9.13 x10^{-5}	31.1	100.6	-	-	75.1	0.00052
	50	13.4	0.9	9.91 x10^{-5}	36.8	109.5	-	-	77.2	0.00086
	100	14.1	0.9	1.09 x10^{-4}	41.5	113.5	-	-	78.0	0.00078
	200	14.6	0.9	1.05 x10^{-4}	43.3	118.0	-	-	78.8	0.00055
MTBT-F	10	1.1	0.9	1.86 x10^{-4}	47.0	54.4	-	-	54.1	0.00245
	15	1.2	0.9	1.83 x10^{-4}	41.2	54.7	-	-	54.3	0.00122
	20	1.2	0.8	1.85 x10^{-4}	37.0	190.9	-	-	86.9	0.00119
	25	1.2	0.8	1.89 x10^{-4}	38.0	215.5	-	-	88.4	0.00154
	30	1.2	0.8	2.00 x10^{-4}	36.2	222.1	-	-	88.7	0.00164
	50	1.2	0.8	2.09 x10^{-4}	39.8	244.5	-	-	89.8	0.00142
	100	1.3	0.8	2.33 x10^{-4}	39.9	251.6	-	-	90.1	0.00302
	200	1.3	0.8	2.34 x10^{-4}	43.7	229.8	-	-	89.1	0.00158
MTBT-Cl	10	1.1	0.9	4.88 x10^{-5}	18.9	190.2	8.69 x10^{-4}	22.7	46.2	0.00319
	15	1.1	0.9	4.83 x10^{-5}	21.0	148.2	3.78 x10^{-3}	18.2	83.1	0.00108
	20	1.0	0.9	5.03 x10^{-5}	25.2	174.1	3.42 x10^{-4}	12.7	85.6	0.00093
	25	1.1	0.9	6.53 x10^{-5}	28.0	166.6	5.48 x10^{-4}	6.3	85.0	0.00114
	30	1.1	0.9	7.43 x10^{-5}	32.5	173.7	6.55 x10^{-4}	10.7	85.6	0.00033
	50	1.2	0.9	1.36 x10^{-4}	60.5	111.7	1.82 x10^{-4}	3.7	60.2	0.00043
	100	1.3	1.0	3.90 x10^{-5}	39.0	99.5	1.20 x10^{-4}	10.2	74.9	0.00041
	200	1.3	0.9	1.22 x10^{-4}	46.1	88.3	1.56 x10^{-3}	8.8	71.7	0.00064
MTBT-Br	10	3.0	0.9	3.99 x10^{-5}	15.2	161.2	6.18 x10^{-4}	-	84.5	0.00044
	15	2.5	0.8	4.25 x10^{-5}	4.3	283.9	7.91 x10^{-4}	27.2	91.2	0.00086
	20	1.5	0.8	4.72 x10^{-5}	4.3	423.1	6.35 x10^{-4}	44.3	94.1	0.00065
	25	1.5	0.8	4.57 x10^{-5}	4.2	445.7	7.84 x10^{-4}	43.5	94.4	0.00055
	30	1.5	0.9	4.86 x10^{-5}	15.0	425.1	8.39 x10^{-4}	60.0	94.1	0.00038
	50	1.6	0.9	4.62 x10^{-5}	15.9	547.0	9.88 x10^{-4}	51.3	95.4	0.00062
	100	1.6	0.9	5.27 x10^{-5}	16.0	610.0	9.48 x10^{-4}	65.8	95.9	0.00043
	200	1.8	0.9	6.23 x10^{-5}	16.9	579.5	9.83 x10^{-4}	70.8	95.7	0.00036
MTBT-I	10	6.5	0.8	7.21 x10^{-5}	10.6	116.1	-	-	78.5	0.00144
	15	6.6	0.8	9.98 x10^{-5}	11.1	140.0	-	-	82.1	0.00242
	20	6.6	0.8	6.83 x10^{-5}	11.6	151.3	-	-	83.5	0.00225
	25	7.1	0.8	7.94 x10^{-5}	10.8	170.4	-	-	85.3	0.00176
	30	7.3	0.8	7.61 x10^{-5}	11.6	164.7	-	-	84.8	0.00279
	50	7.6	0.8	8.88 x10^{-5}	12.7	177.9	-	-	85.9	0.00397
	100	7.7	0.8	7.62 x10^{-5}	11.8	227.4	-	-	89.0	0.00588
	200	7.5	0.8	7.36 x10^{-5}	11.2	261.0	-	-	90.4	0.00534

3.2 Thermodynamic Analysis

The adsorption mechanisms of organic compounds reported in the literature involve studies using adsorption isotherms, including works from Frumkin, Langmuir, Temkin and Freundlich [46-

49]. These studies contain the common parameter, the degree of cover, which is related to the inhibition efficiency using equation (4):

$$\theta = \frac{\eta}{100} \quad (4)$$

In the plot of $C\Theta^{-1}$ vs C as shown in Figs. 6a and 6b, the red line presents a linear adjustment that responds to the Langmuir isotherm and is represented by equation (5):

$$\frac{C}{\theta} = \frac{1}{k_{\text{ads}}} + C \quad (5)$$

where C = concentration (mol/L), k_{ads}= adsorption constant (mol/L).

However, the adsorption constant is related to the Gibbs standard energy ($\Delta G°_{ads}$), which can be calculated with:

$$\Delta G°_{\text{ads}} = -RT \ln 55.5 k_{\text{ads}} \quad (6)$$

where R is the gas constant and T is the absolute temperature (K). The concentration of water in solution in mol L^{-1} is 55.5.

The values of ln(k_{ads}) and $\Delta G°_{ads}$ provide insight into the adsorption mechanism. Values higher than -20 KJ/mol indicate a physisorption process for the inhibitors due to an electrostatic interaction between the molecule and the charged surface [50]. In contrast, values higher than -40 KJ/mol indicate a chemisorption process [51-52].

These parameters are summarized in Table 3. It should be noted that all the monotriazoles derived from uracil and thymine exhibited a $\Delta G°_{ads}$ between -20 KJ/mol and -40 KJ/mol, which indicates the simultaneous physical and chemical adsorption of these molecules on the mild steel surface from the H_2SO_4 with predominantly physical absorption [53-55].

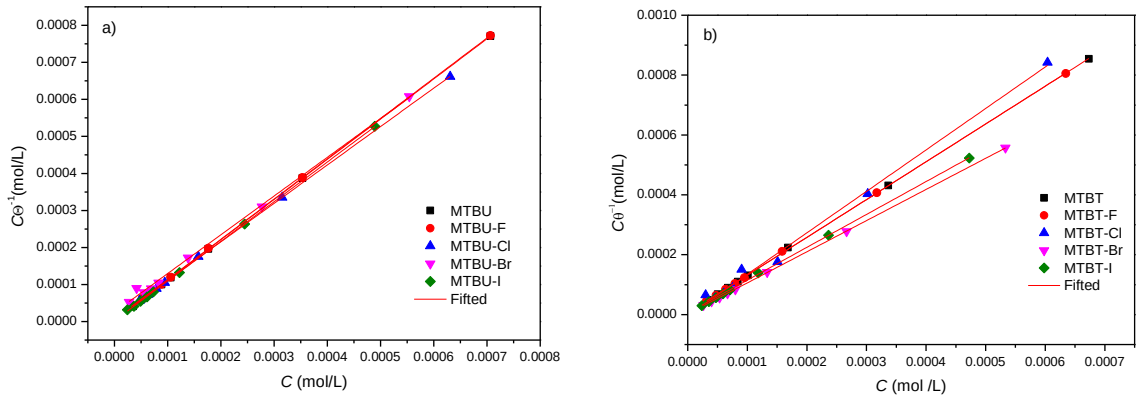

Figure 6. Adsorption isotherm at different concentrations of MTBU and MTBT derivatives on API 5L X52 steel immersed in 1 M H_2SO_4

Table 3. Electrochemical parameters of MTBU and MTBT derivatives determined by the Langmuir isotherms

Compound	lnk_{ads}	$\Delta G°_{ads}$ (KJ/mol)	Compound	Lnk_{ads}	$\Delta G°_{ads}$ (KJ/mol)
MTBU	16.44	-37.34	**MTBT**	16.04	-36.42
MTBU-F	16.22	-36.84	**MTBT-F**	16.22	-36.84
MTBU-Cl	15.75	-35.77	**MTBT-Cl**	16.44	-37.34
MTBU-Br	14.43	-32.77	**MTBT-Br**	17.13	-38.92
MTBU-I	17.13	-38.92	**MTBT-I**	16.22	-36.84

3.3. Rotation rate effect

To assess the conditions under which the hydrocarbons are transported (laminar or turbulent flow) according to the ASTM G170 and ASTM G-185 standards, the best inhibitor of each family was tested under laminar flow conditions.

In Fig. 1s, the impedance diagrams obtained at two rotation rates are shown for different concentrations of the inhibitor. Figs. 1s(a) and (b) correspond to the moment at which the MTBU-I was gradually added to the corrosive medium. Comparing the diagrams, it is observed that the diameter of the semicircle increases for concentrations from 50 ppm to 200 ppm at a rotation rate of 100 rpm. When the MTBT-Br was evaluated, a continuous increase in the value of Z_{re} was observed with the increasing concentration of the inhibitor, presenting similar behaviors at both rotation rates. Two time constants were observed, and the Nyquist diagrams indicate that one time constant at high frequencies is attributed to the formation of a film composed of the corrosion products that the inhibitor molecules are attached, while the second time constant, a semicircle at low frequencies, is attributed to the charge transfer resistance in the pores or defects of the film formed by the corrosion products [56].

Table 4 shows the characteristic parameters obtained from the experimental data with the equivalent electric circuits shown in Fig. 1s. For both evaluated compounds, R_{ct} increases with the increasing concentration at both rotation rates. For the MTBU-I, it was observed that the best conditions were at 40 rpm because the efficiencies are greater than 80% from concentrations greater than 20 ppm. This suggests that this compound has a quicker adsorption-desorption process at higher rotation rates [57]. The MTBT-Br shows good protection against corrosion for both 40 and 100 rpm at concentrations greater than 15 ppm, with η values greater than 85%. This result can be attributed to the fact that apart from having a halogen in its chemical structure, the MTBT-Br contains a methyl group, which is an important structural feature to decrease the corrosion of metallic surfaces [58]. This indicates that under static conditions, both compounds exhibit some degree of inhibition efficiency.

However, under laminar flow conditions, increased protection against corrosion is observed for inhibitor concentrations above 50 ppm.

Table 4 Adjustment parameters of different concentrations of MTBU-I and MTBT-Br obtained at 40 and 100 rpm

Inhibitor	Rotation rate (rpm)	*C* (ppm)	R_s (Ω cm^2)	α	*Q* (S sec^α)	R_{ct} (Ω cm^2)	*Q* (S sec^α)	R_{mol} (Ω cm^2)	η (%)
MTBU-I	40	10	0.70	1.00	1.75 x10^{-5}	139.1	-	-	78.4
		15	0.70	1.00	1.77 x10^{-5}	139.1	-	-	78.4
		20	0.72	1.00	1.09 x10^{-5}	145.6	-	-	79.4
		50	4.45	1.00	9.64 x10^{-6}	224.0	2.10 x10^{-4}	16.9	87.5
		100	1.51	0.70	1.48 x10^{-4}	280.4	6.23 x10^{-4}	15.6	89.9
	100	10	0.70	1.00	2.01 x10^{-5}	94.8	-	-	68.4
		15	0.99	1.00	2.31 x10^{-5}	136.6	-	-	78.0
		20	1.03	1.00	1.61 x10^{-5}	130.0	-	-	76.9
		50	1.77	0.98	1.03 x10^{-5}	223.8	1.54 x10^{-4}	5.8	86.6
		100	1.71	1.00	3.92 x10^{-6}	309.5	2.54 x10^{-4}	3.5	90.3
MTBT-Br	40	10	10.1	0.91	3.31 x10^{-5}	125.7	-	-	80.1
		15	11.99	0.92	3.78 x10^{-5}	143.6	-	-	82.5
		20	13.57	0.94	4.74 x10^{-5}	127.6	-	-	80.4
		50	14.78	0.93	9.93 x10^{-5}	131.9	-	-	81.0
		100	12.26	0.93	1.10 x10^{-4}	146	-	-	82.8
	100	10	8.64	0.91	4.83 x10^{-5}	105.00	-	-	76.1
		15	14.96	0.96	3.45 x10^{-5}	165.10	-	-	84.8
		20	15.91	0.93	4.84 x10^{-5}	159.30	-	-	84.3
		50	16.95	0.93	9.10 x10^{-5}	170.00	-	-	85.2

Table 5. Parameters obtained for different immersion times and static conditions of the MTBU-I and MTBT-Br

Inhibitor	Immersion Time (h)	R_s (Ω cm^2)	α	*Q* (S sec^α)	R_{ct} (Ω cm^2)	*Q* (S sec^α)	R_{mol} (Ω cm^2)	η (%)	*X*
MTBU-I	**0.5**	0.7	0.9	2.11 x10^{-4}	360.0	6.01 x10^{-5}	77.5	94.3	0.00051
	1	1.1	1.0	1.30 x10^{-4}	681.5	9.74 x10^{-6}	2.3	96.3	0.00056
	24	1.0	0.9	1.50 x10^{-4}	507.1	4.27 x10^{-5}	109.1	95.9	0.00051
	48	3.0	0.8	1.72 x10^{-4}	322.7	2.31 x10^{-5}	15.5	92.6	0.00077
	72	2.6	0.9	2.18 x10^{-5}	271.4	1.96 x10^{-5}	11.2	91.2	0.00130
	120	2.0	0.9	2.73 x10^{-4}	217.2	2.45 x10^{-4}	8.9	88.9	0.00130
	168	0.8	0.8	1.99 x10^{-3}	45.1	5.16 x10^{-4}	4.1	49.2	0.00045
	240	2.5	0.9	2.69 x10^{-3}	28.3	3.26 x10^{-3}	6.9	28.9	0.00100
MTBT-Br	**0.5**	1.5	0.8	4.57 x10^{-5}	445.7	7.84 x10^{-4}	43.5	94.4	0.00055
	1	6.5	0.9	1.56 x10^{-5}	443.8	1.11 x10^{-5}	0.9	94.4	0.00057
	24	6.8	0.8	3.07 x10^{-4}	210.9	4.05 x10^{-5}	45.0	90.2	0.00601
	48	6.4	0.7	2.81 x10^{-4}	219.7	2.43 x10^{-4}	31.3	90.0	0.00077
	120	9.1	0.8	1.25 x10^{-4}	71.5	5.56 x10^{-4}	4.3	67.0	0.00036
	168	0.7	0.7	2.19 x10^{-3}	68.1	1.14 x10^{-3}	19.3	71.4	0.00212
	240	0.5	0.8	1.97 x10^{-6}	76.4	3.90 x10^{-6}	0.4	67.4	0.00196

Another important parameter to consider regarding the efficiency of the corrosion inhibitors is the durability of the film formed by the chemical compound according to the ASTM G48 or G78.

Table 5 shows the results corresponding to different immersion times of MTBU-I and MTBT-Br at 50 ppm. For the MTBU-I, the value of R_p increases immediately following immersion and then gradually decreases over time to 306.8 Ωcm^2 after 72 hours. On the other hand, the value R_p of the MTBT-Br decreased to 231.2 Ω cm^2 after 48 h. In both cases, the decreased polarization resistance over time can be attributed to the deterioration of the protective layer of the inhibitor. This suggests that the protective film formed by the inhibitor is not compact enough to provide corrosion resistance over long immersion periods [59-61].

However, the MTBT-Br offers a superior η over time compared to the MTBU-I. This is because the former loses its inhibition performance gradually up to 250 hours of immersion, with the η remaining above 70%.

3.4 Characterization by SEM-EDS

SEM images of the metal surface are shown in Fig. 7 revealing differences in the roughness resulting from having surface treatment or not. Fig. 7a corresponds to the polished surface, while Fig. 7b shows the metal surface after 24 hours of immersion in 1 M H_2SO_4, revealing the effects of the damage imparted by the corrosive medium. In contrast, Figs. 7c and 7d correspond to the metal surface in the presence of the inhibitors MTBU-I and MTBT-Br, respectively, and shows that the corrosive effects are proportionally lower due to film formation of the inhibitor on the metallic surface.

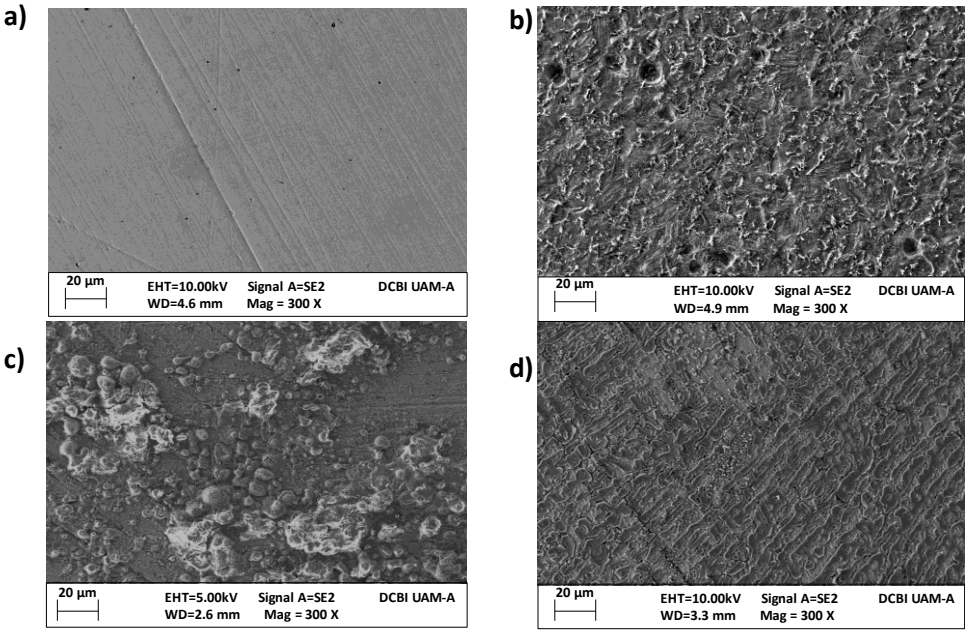

Figure 7. SEM images of steel that is a) polished, b) immersed in H_2SO_4, c) with MTBU-I and d) with MTBT-Br

4. CONCLUSIONS

Evaluation of the inhibition efficiency of the MTBU derivatives as corrosion inhibitors for API 5L X52 steel in 1 M H_2SO_4 shows the following trend:

MTBU-I > MTBU-F > MTBU-Cl> MTBU-Br

Furthermore, the best performer of the monotriazoles derived from thymine that were investigated was the MTBT-Br.

The adsorption process associated with the investigated molecules was determined to be a simultaneous physisorption-chemisorption process, as described by the Langmuir isotherms.

A study of the immersion time demonstrated that the monotriazoles derived from uracil with bromide (MTBU-Br) provides a moderately effective corrosion inhibition after 250 hours, with an η of ~77%.

ACKNOWLEDGMENTS

AEV and FJRG express their gratitude to the Facultad de Química (UNAM), Departamento de Ingeniería Metalúrgica and CONACyT for providing a postdoctoral fellowship.

We wish to acknowledge the SNI (Sistema Nacional de Investigadores) for the distinction of their membership and the stipend received.

We thank the Divisional Electronic Microscopy Lab (Laboratorio Divisional de Microscopía Electrónica) for the use of the SUPRA 55 VP.

References

1. I. Lozano, E. Mazario, C.O. Olivares, N.V. Likhanova and P. Herrast, *Mat. Chem. Phys.,* 147 (2014) 191.
2. A.M. Al-Turkustani, S.T. Arab and L.S.S Al-Qarni, *J. Sau.Chem. Soc.,* 15 (2011) 73.
3. M. Znini, L. Majidi, A. Bouyanzer, J. PaoliniJ, J. M. Desjobert, J. Costa and B. Hammoutoi, *Arab. J. Chem.,* 5 (2012) 467.
4. K. R. Ansari and M.A. Quraishi, *J. Taiwan Inst. Chem. E.,* 54 (2015) 145.
5. J. Bhawsar, P.K. Jain and P. Jain, *Alex. Eng. J.,* 54 (2015) 769.
6. M.M. Hamza, S.S. Abd El Rehim and A.M. Ibrahim, *Arab. J. Chem.,* 6(2013) 413.
7. E. Stupnisek, A. Gazivoda and M. Madzarac, *Electrochim. Acta*, 47(2002) 4189.
8. M.G. Hosseini, M. Ehteshamzadeh and T. Shahrabi, *Electrochim. Acta,* 52 (2007) 3680.
9. S. Ghareba, S. Omanovic, *Electrochim. Acta,* 56 (2011) 3890.
10. C. Jeyaprabha, S. Sathiyanarayanan and G. Venkatachari, *Electrochim. Acta,* 51 (2006) 4080.
11. X. Li, S. Deng and H. Fu, *Corros. Sci.,* 53 (2011) 3241.
12. J. Saranya, M. Sowmiya, P. Sounthari, K. Parameswari, S. Chitra and K. Senthilkumar, *J. Mol. Liq*., 216 (2016) 42.
13. A. Pourghasemi, R. Naderi, E. Kowsari and M. Sayebani, *Corros. Sci*., 107 (2016) 96.
14. Hejazi, S.H. Mohajernia, M.H. Moayed, A. Davoodi, M. Rahimizadeh, M. Momeni, A. Eslami, A. Shiri and A. Kosari*, J. Ind. Eng. Chem.,* 25 (2015) 112.
15. P. Mourya, P. Singh, R.B. Rastogi and M.M. Singh, *Appl. Surf. Sci.,* 380 (2016) 14.
16. M. Mehdipour, R. Naderi and B.P. Markhali, *Prog. Org. Coat.,* 77 (2014) 1761.

17. A. Kadhim, A.K. Al-Okbi, D.M. Jamil, A. Qussay, A.A. Al-Amiery, T. Sumer, A.A. Kadhum, A.B. Mohamad and M.H. Nassir, *Results Phys*., 7 (2017) 4013.
18. N. Chafai, S. Chafaa, K. Benbouguerra, D. Daoud, A. Hellal and M. Mehri, *J. Taiwan Inst. Chem. E.,* 70 (2017) 331.
19. K.R. Ansari, M.A. Quraishi and A. Singh, *Corros. Sci*., 95 (2015) 62.
20. K. Zakaria, N. A. Negm, E.A. Khamis and E.A. Badr, *J. Taiwan Inst. Chem. E.,* 61 (2016) 316.
21. I.B. Obot, N.O. Obi-Egbedi and N.W. Odozi, *Corros. Sci.,* 52 (2010) 923-926.
22. M. Bouklah, B. Hammouti, A. Aouniti and T. Benhadda, *Prog. Org. Coat.,* 49 (2004) 225.
23. A. Döner, G. Kardas, *Corros. Sci*., 53 (2011) 4223.
24. A. Ouchrif, M. Zegmout, B. Hammouti, A. Dafali, M. Benkaddour, A. Ramdani and S. Elkadiri, *Prog. Org. Coat.,* 53 (2005) 292.
25. S.M. Salih, A.H. Hussien, *J. Mol. Struc*., 1076 (2014) 658.
26. J. Tan, L. Guo and S. Xu, *J. Ind. Eng.Chem.,* 25 (2015) 295.
27. A. Espinoza, G.E. Negrón, R. González, D. Ángeles, H. Herrera, M. Romero and M. Palomar, *Mat. Chem. Phys.,* 145 (2014) 407.
28. Q. Deng, N. Ding, X. Wei, L. Cai, X. Peng He, L. Long, G. Gong and K. Chen, *Corros. Sci.,* 64 (2012) 64.
29. Q. Deng, H. Shi, N. Ding, B. Chen, X. He, G. Liu, Y. Tang, Y. Long and G. Chen, *Corros. Sci*., 57 (2012) 220.
30. H. Zhang, X. He, Q. Deng, Y. Long, G. Chen and K. Chen, *Carbohydr. Res.,* 354 (2012) 32.
31. Q. Deng, X. He, H. Shi, B. Chen, G. Liu, Y. Tang, Y. Long, G. Chen and K. Chen, *Ind. Eng. Chem. Res.,* 51 (2012) 7160.
32. T. Zhang, S. Cao, H. Quan, Z. Huang and S. Xu, *Res. Chem. Intermed.,* 41(2015) 2709.
33. B. Ramaganthan, M. Gopiraman, L. Olasunkanmi, M. Kabanda, S. Yesudass, I. Bahadur, A. Adekunle, I. Obot and E. Ebenso, *RSC Adv.,* 5 (2015) 76675.
34. R. González, A. Espinoza, G.E. Negrón, M.E. Palomar, M.A. Romero and R. Santillán, *Molecules,* 18 (2013) 15064.
35. A. Espinoza, F. Rodríguez, R. González, D. Ángeles, D. Mendoza and G.E. Negrón, *RSC Adv.,* 6 (2016) 72885.
36. S. Zhang, Z. Tao, W. Li and B. Hou, *Appl. Surf. Sci*., 255 (2009) 6757.
37. L. Afia, N. Rezki, M.R. Aouad, A. Zarrouk, H. Zarrok, R. Salghi, B. Hammouti, M. Messali and S.S. Al-Deyab, *Int. J. Elec. Sci.,* 8 (2013) 4346.
38. A. Zarrouk, B. Hammouti, S. S. Al-Deyab, R. Salghi, H. Zarrok, C. Jama and F. Bentiss, *Int. J. Elec. Sci.,* 7 (2012) 5997.
39. R. Solmaz, *Corros. Sci.,* 81 (2014) 75.
40. G. J. Brug, Van Den AIG, *J. Electroanal. Chem. and Int. Electrochem.,* 176 (1984) 275.
41. R. Solmaz, E. Altunbas, A. Doner and G. Kardas, *Corros. Sci.,* 53 (2011) 3231.
42. N. Kumar, C. Verma, M. A. Quraishi and A. K. Mulherjee, *J. Mol. Liq.,* 215 (2016) 47.
43. A. Khamis, M.M. Saleh, M.I. Awad and B.E. El-Anadouli, *J. Adv. Res.,* 5 (2014) 637.
44. K. Zhang, B. Xu, W. Yang, X. Yin, Y. Liu and Chen, *Corros. Sci*., 90 (2015) 284.
45. Q. Sudheer, K. Ansari and E. Ebenso, *Int. J. Elec. Sci*., 7 (2012) 7476.
46. L. Malki, B. Hammouti, A. Bellaouchou, A. Benbachir, A. Guenbour and S. Kertit, *Der. Pharm.,* 3 (2011) 353-360.
47. Z. Tao, W. He, S. Wang, S. Zhang and G. Zhou, *Corros. Sci*., 60 (2012) 205.
48. Zarrouk, B. Hammouti, H. Zarrok, M. Bouachrine, K.F. Khaled and S.S. Al-Deyab, *Int. J. Electrochem. Sci.,* 7 (2012) 89.
49. F. Xu, J. Duan, S. Zhang and B. Hou, *Mat. Lett*., 62 (2008) 4072.
50. M. El-Sayed, *Int. J. Electrochem. Sci.,* 7 (2012) 1482.
51. Y.H. Ahmad, A. S. Mogoda and A.G. Gadallh, *Int. J. Electrochem. Sci.,* 7 (2012) 4929.
52. M.K. Pavithra, T.V. Venkatesha, M.K. Punith and H.C. Tondan, *Corros. Sci*., 60 (2012) 104.

53. W. Chen, H. Qun and L.N. Bing, *Corros. Sci.,* 53 (2011) 3356.
54. R. Solmaz, *Corros. Sci.,* 79 (2014) 169.
55. R. Solmaz, G. Kardas, B. Yazici and M. Erbil, *Colloids and Surfaces A,* 312 (1) (2008) 7.
56. G.H. Golestani, M. Shahidi and D. Ghazanfari, *App Surf. Sci.,* (2014) 347.
57. A. Espinoza and F.J. Rodríguez, *RSC adv.,* 6 (2016) 70226.
58. A. Espinoza, G.E. Negrón, D. Ángeles, M.E. Palomar, M.A. Romero and H. Herrera, *ECS Transactions,* 36 (2011) 217.
59. C.B. Verma, M.A. Quraishia and A. Singh, *J. Taiwan Inst. Chem. E.,* 49 (2015) 229.
60. P.D. Reena, J. Nayak and A. Nityananda, *Port. Electrochim. Acta,* 29 (2011) 445.
61. T. Chieb, K. Belmokre, M. Benmessaoud, S. El Hassane, N. Hajjaji and A. Srhiri, *Mat. Sci. Appl.,* 2 (2011) 1260.